A Multi-Criteria Decision-Making Optimization Model for Flood Management in Reservoirs

1st Author

Banafsheh Nematollahi

Ph.D., Department of Civil and Environmental Engineering, Shiraz University, Shiraz, Iran. Email Address: b.Nematollahi@shirazu.ac.ir

2nd Author (Corresponding Author)

Mohammad Reza Nikoo

Associate Professor, Department of Civil and Architectural Engineering, Sultan Qaboos University, Muscat, Oman. Email Address: m.reza@squ.edu.om

3rd Author

Amir H. Gandomi

Professor, Faculty of Engineering and Information Technology, University of Technology Sydney, Ultimo, Australia. Email Address: gandomi@uts.edu.au

4th Author

Nasser Talebbeydokhti

Professor, Department of Civil and Environmental Engineering, Head of Environmental Research and Sustainable Development Center, Shiraz University, Shiraz, Iran. Email Address: taleb@shirazu.ac.ir

5th Author

Gholam Reza Rakhshandehroo

Professor, Department of Civil and Environmental Engineering, Shiraz University, Shiraz, Iran. Email Address: rakhshan@shirazu.ac.ir

A Multi-Criteria Decision-Making Optimization Model for Flood Management in Reservoirs

Banafsheh Nematollahi[1], Mohammad Reza Nikoo[2*], Amir H. Gandomi[3], Nasser Talebbeydokhti[4], Gholam Reza Rakhshandehroo[5],

Abstract

Flood management in a reservoir-outlet system is a multi-criterion decision-making (MCDM) issue, in which preventing flood damage and flood overtopping, as well as fulfilling water demands, are often considered essential practices. However, although MCDM models can be used for flood control, there is a knowledge gap in hybrid modeling of the reservoirs and their outlets based on a coupled MCDM and optimization model during the flood. In this paper, an MCDM-optimization model was presented for reservoir systems' optimal designs in flood conditions based on a robust optimization technique, namely multi-objective particle swarm optimization (MOPSO), applying a powerful MCDM tool, so-called complex proportional assessment (COPRAS) for the first time in the literature, considering the weights generated by Shannon Entropy method. The objectives of this optimization model were defined based on the non-linear interval number programming (NINP) technique to optimize the orifice and triangular, rectangular, and proportional weirs specifications. This methodology was applied to a practical reservoir MCDM optimization problem in flood conditions to demonstrate its applicability and

[1] PhD, Department of Civil and Environmental Engineering, Shiraz University, Shiraz, Iran.

[2*] Associate Professor, Department of Civil and Architectural Engineering, Sultan Qaboos University, Muscat, Oman. Email Address: m.reza@squ.edu.om.

[3] Professor, Faculty of Engineering and Information Technology, University of Technology Sydney, Ultimo, Australia.

[4] Professor, Department of Civil and Environmental Engineering, Head of Environmental Research and Sustainable Development Center, Shiraz University, Shiraz, Iran.

[5] Professor, Department of Civil and Environmental Engineering, Shiraz University, Shiraz, Iran.

efficiency. Results indicated that the proposed framework could successfully and effectually provide the reservoirs and outlets with superior optimal design.

Keywords: Flood management, Multi-objective particle swarm optimization (MOPSO) model, Non-linear interval number programming (NINP) method, Complex proportional assessment (COPRAS) technique, Shannon Entropy method.

1 Introduction

Flood management plays a prominent role in water engineering due to substantial flood destruction to people's lives (Jacob et al. 2019). The key variables governing flood management are providing the reservoir's safety, preventing downstream flood damages, and fulfilling the water demands requirements. However, balancing different profit-making goals is still challenging to obtain optimal extensive benefits in flood conditions (Eldardiry and Hossain 2021). Therefore, intelligent optimization algorithms should be applied to provide optimum reservoirs and outlet specifications during floods (Yazdandoost 2021).

Recently, several heuristic intelligent techniques such as ant colony algorithm (ACO) (Gang et al. 2005), simulated annealing algorithm (SA), genetic algorithm (GA) (Jothiprakash and Arunkumar 2013), particle swarm optimization (PSO) (Chen et al. 2020), and multi-objective optimization models (Wang et al. 2011; Su and Tung 2014) have been utilized to optimize reservoir characterizations. However, among these techniques, although some studies considered outlets optimal designs within the reservoir operation optimization in flood conditions (Karaboga et al. 2004; Karaboga et al. 2008), they have been paid less attention. On the other hand, multi-objective particle swarm optimization (MOPSO) is an effective algorithm using swarm intelligence that can fill this knowledge gap due to its advantages over other approaches, such as easy understanding of procedure and programming (Shuai and Huang Xiaomin 2012). As a result, applying the MOPSO optimization technique for optimal reservoirs and outlet designs in flood conditions can be a substantial achievement in water engineering.

For a MOPSO optimization model, it is not feasible to define a single optimum alternative that optimizes all objective functions since some of the objectives may conflict with each other (Malekmohammadi et al. 2011; Zhu et al. 2016); on the other hand, it is more suitable to choose the most appropriate and superior alternative from a set of possible options (Yu et al. 2004), so that, selecting the superior optimum result of the MOPSO model is a multi-criterion decision-making (MCDM) issue. Several types of MCDM tools have been studied in the literature for reservoir flood control and risk management using different approaches (Brito and Evers 2016), including fuzzy recognition model (Chen and Hou 2004), Technique for Order Preference by Similarity to Ideal Solution (TOPSIS) (Fu 2008), analytic hierarchy process (AHP) (Alipour 2015), and goal programming (Mamun et al. 2015). However, to the best of our knowledge, the application of a robust MCDM technique such as the complex proportional assessment (COPRAS) method for ranking the alternatives related to a multi-objective optimization model for the reservoirs and outlets designs in flood conditions has not been addressed in the literature (Ashrafi et al. 2021; Roozbahani et al. 2021). Therefore, using the COPRAS model as a successful MCDM tool coupled with a reservoir optimization model in flood conditions can significantly advance the current use.

This paper proposed a hybrid MCDM-MOPSO model considering the non-linear interval number programming (NINP) technique in the optimization objectives as averages and radii of flood overtopping, downstream water deficit, and flood damage as well as outlets characteristics involving the COPRAS approach as an MCDM tool using Shannon Entropy method for generating the weights to obtain the superior optimal designs of the reservoirs outlets. This novel methodology endeavored to fulfill the objectives elaborated upon hereunder to introduce the superior, reliable, optimum design of the reservoirs and their outlets;

1. Minimize the downstream water deficit, flood overtopping, and flood damage based on the NINP approach,
2. Optimize the reservoir's outlets' characterizations using several flood inflow scenarios using five common inflow patterns abrupt wave, triangular, broad peak, flood pulse, and double-peak,
3. Develop a novel optimization model for optimal designs of four outlet types of orifice and triangular, rectangular, and proportional weirs within a MOPSO optimization model,
4. Adopt the COPRAS approach to find the most appropriate optimal solution,
5. Use the Shannon Entropy method to generate the importance weights related to different objectives,
6. Manage the flood by optimizing reservoirs and outlet designs while considering the downstream water demands during the floods.

2 Methodology

The proposed framework consisted of five primary steps for obtaining the superior optimal outlets' designs using the MOPSO model based on modified Euler's method as a well-known Runge-Kutta scheme considering the NINP technique for uncertainties evaluations and a robust MCDM model, the COPRAS tool for ranking alternatives using Shannon Entropy for generating the importance weights (Fig. 1).

First, different flood hydrograph scenarios were generated based on five common inflow types: Flood pulse, abrupt wave, broad peak, double-peak, and triangular by variations in durations of the flood and peak of the inflows.

Second, the flood routing equations using four conventional outlet types of triangular, proportional, and rectangular weirs and orifice were formulated and solved numerically by the modified Euler's method (Badfar et al. 2021).

Third, the MOPSO model was developed to optimize different outlets features, which resulted in a series of Pareto-optimal solutions between different objectives of radii and averages of flood overtopping, flood damage, and water demand deficit as well as outlets characteristics using the water demand and the inflow scenarios as the input.

Fourth, the weights related to objectives were computed using the Shannon Entropy method based on each objective's deviation degree and the Entropy.

Finally, the COPRAS decision-making approach was applied to rank the optimal solutions by computing the utilities for each alternative and selecting the solution with the highest utility as the final superior optimum result. These steps were delineated entirely in the following.

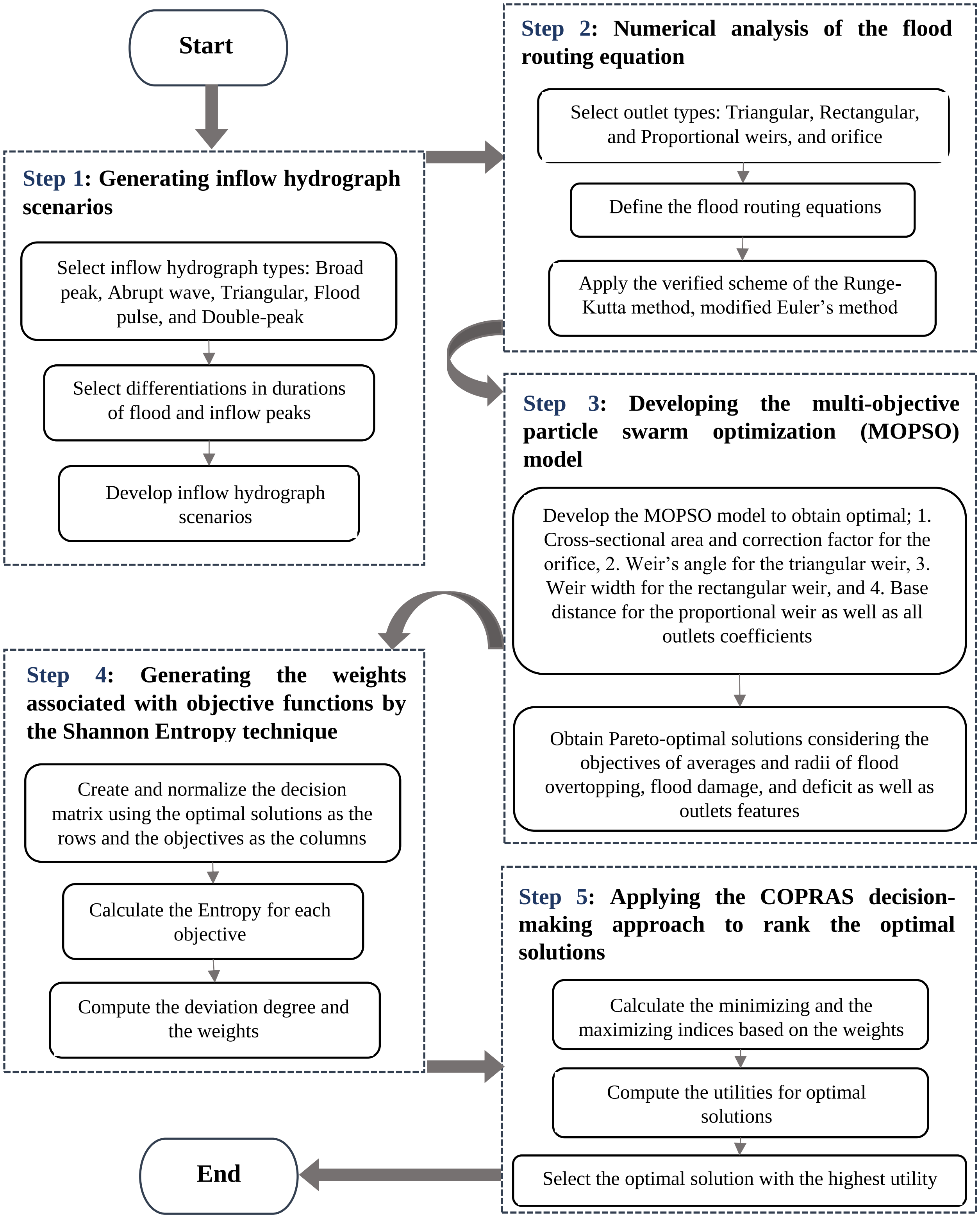

Fig. 1 The general framework for the presented hybrid MCDM-MOPSO model

2.1 Inflow hydrographs

In this research, fifty flood hydrographs, ten of each primary pattern as double-peak, broad peak, flood pulse, triangular, and abrupt wave, were developed by variations in flood durations and peak inflows (Fig. 2) (Paik 2008; Nematollahi et al. 2021). In other words, four types of the hydrograph, broad peak, triangular, flood pulse, and abrupt wave were considered using a thesis by Hui (2013); in addition, to cover almost all inflow hydrographs for floods in the simplified shapes and the double-peak inflow pattern was adopted from Gioia (2016).

These inflow hydrographs based on the flood durations and the inflow base peaks were obtained from a study by Paik (2008) and utilized as inputs to the optimization model. The inflow peaks and flood durations were different in the inflow flood scenarios to incorporate uncertainties in the duration time of flood and inflow peak, which was essential for the hydrological risk evaluation of reservoir water shortage in the risk-based optimization model.

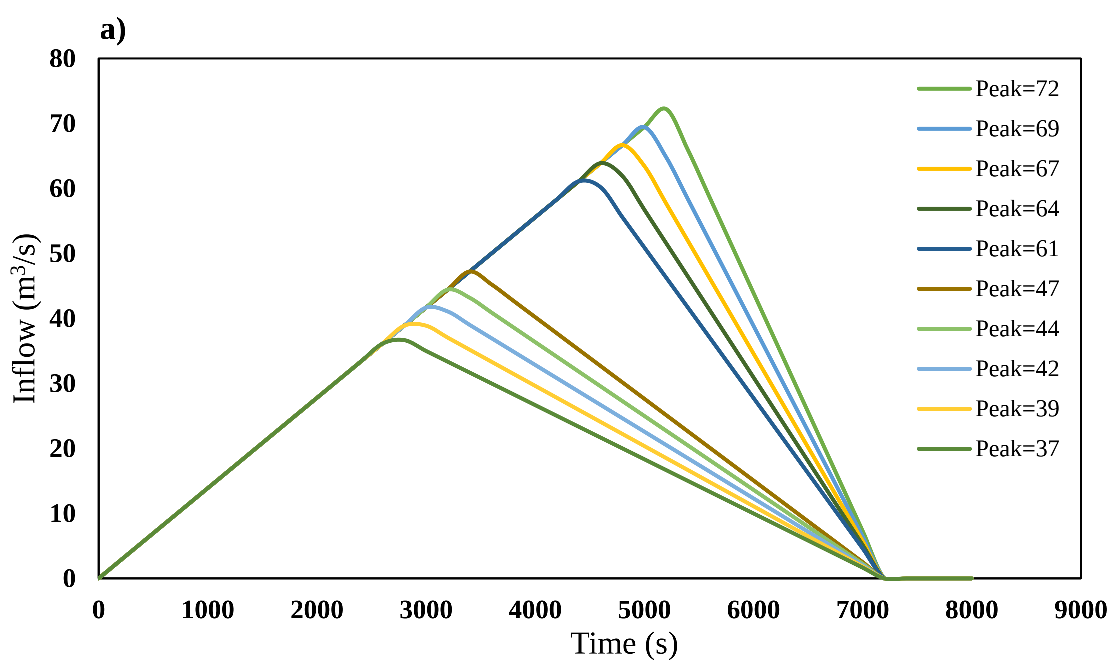

b)

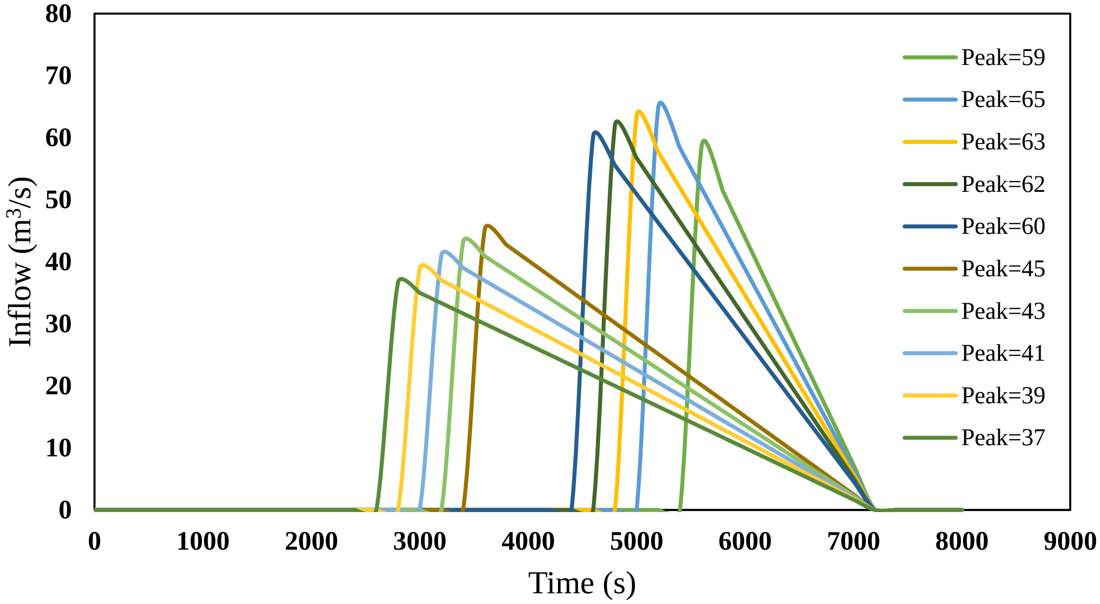
Peak=59
Peak=65
Peak=63
Peak=62
Peak=60
Peak=45
Peak=43
Peak=41
Peak=39
Peak=37
Inflow (m3/s)
Time (s)
0
10
20
30
40
50
60
70
80
0
1000
2000
3000
4000
5000
6000
7000
8000
9000

c)

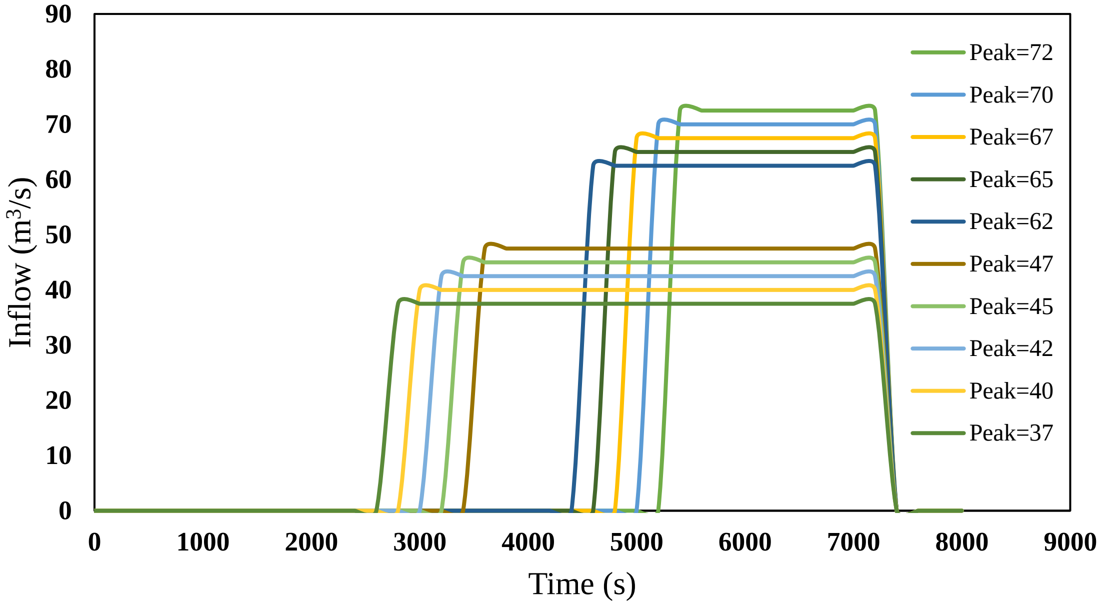
Peak=72
Peak=70
Peak=67
Peak=65
Peak=62
Peak=47
Peak=45
Peak=42
Peak=40
Peak=37
Inflow (m3/s)
Time (s)
0
10
20
30
40
50
60
70
80
90
0
1000
2000
3000
4000
5000
6000
7000
8000
9000

d)

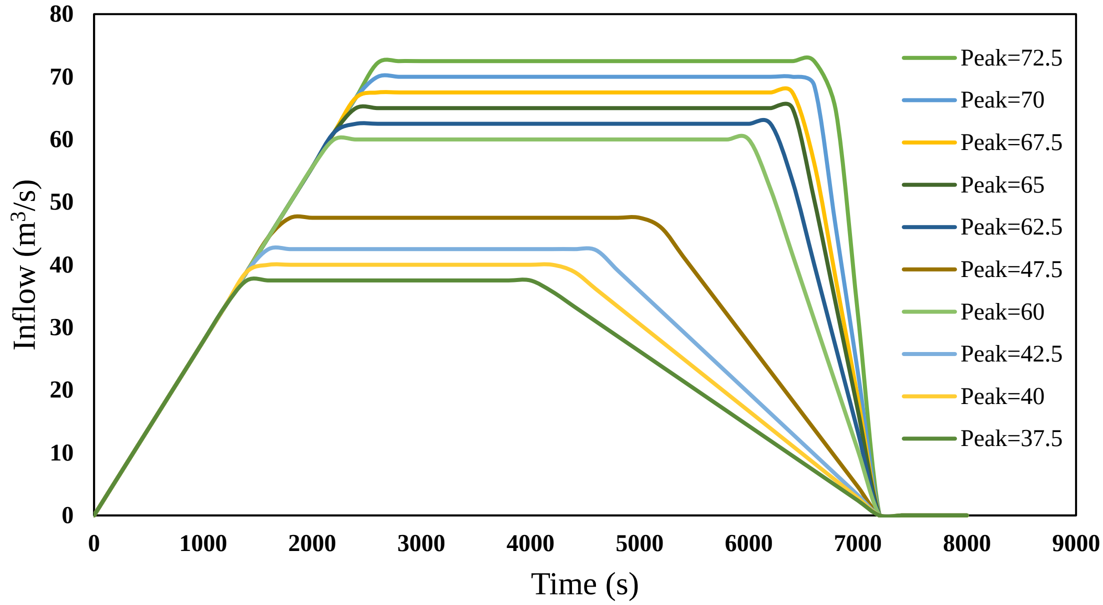

e)

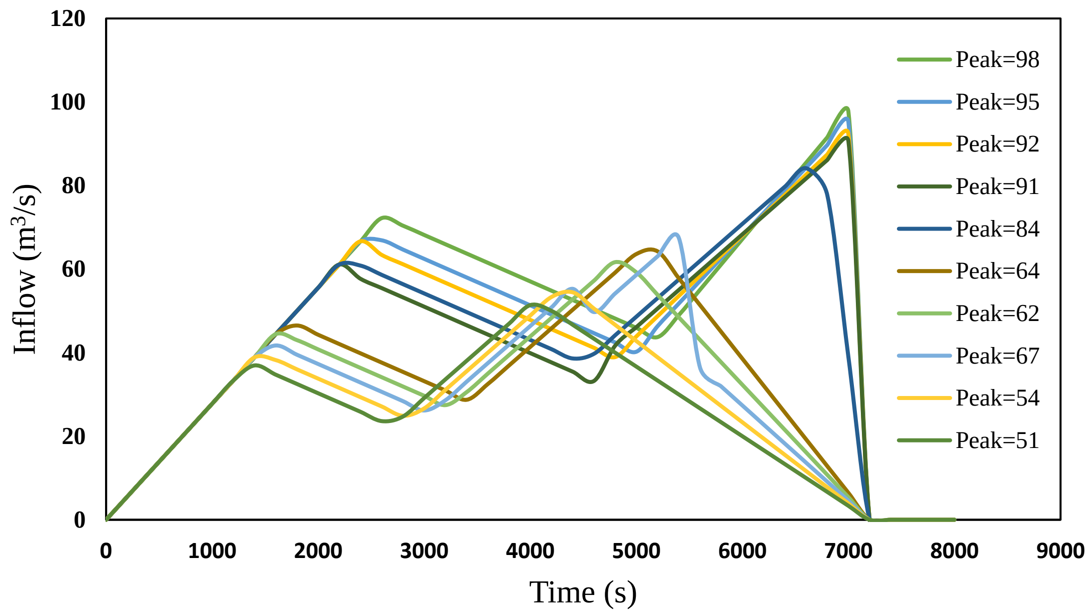

Fig. 2 The inflow hydrographs based on five primary types; a) Triangular, b) Abrupt wave, c) Flood pulse, d) Broad peak, e) Double-peak

2.2 The multi-objective optimization framework

2.2.1 Outlet formulation

Four conventional outlets were utilized in this study as orifice and triangular, rectangular, and proportional weirs. To this extent, rational cross-sections were initially chosen from the study by Paik (2008), hypothesized to be empty. After that, the optimum designs of the outlets were defined by the proposed optimization model using a well-known Runge-Kutta method for numerical analysis of the flood routing equation using Eqs. (S.1) – (S.5) in the Supplementary materials, section S1 for the outflows characterization in the orifice and triangular, rectangular, and proportional weirs, respectively.

2.2.2 Multi-objective particle swarm optimization (MOPSO) algorithm

The multi-objective particle swarm optimization (MOPSO) algorithm is an extended version of the PSO model used in multi-objective optimization algorithms. The MOPSO approach results in a set of non-inferior solutions rather than a unique solution produced by the PSO approach, the so-called "Pareto set" consisting of different Pareto optimal solutions that do not dominate each other with two main features: 1. Each pair of solutions in the Pareto set cannot compare their validity, and 2. Each Pareto set solution should be superior to the outside solution (Sin-Lau et al. 2005). To transfer from PSO algorithm to MOPSO approach, the operations should be updated to *gBest* of particle swarm while setting reasonable diversity maintenance procedure. Further details were provided in the Supplementary materials, section 3 (Shuai and Huang Xiaomin 2012).

2.2.3 Objective Functions

Defining an appropriate objective function is a key to optimization problems for flood management. This study used seven objective functions categorized in two groups of interval-based and cost-based, considering the downstream safety, water demands, and the safety of the reservoirs in flood conditions.

2.2.3.1 Interval-based objective functions

The concept of non-linear interval number programming (NINP) introduced by Jiang et al. (2008) can be applied to an optimization model's objective functions to decrease the impacts of hydrological uncertainties on the optimization model. The NINP technique has the advantage of hypothesizing that the numbers have interval natures by defining the average and deviation of the objectives for each set of functions (Pourshahabi et al. 2020). This study described three sets of interval-based objective functions as Eqs. (1) to (3) to minimize the averages and deviations of the flood overtopping, downstream flood damage, and water demands deficits by applying the NINP method's deterministic type.

$$\begin{cases} F_1 = \min(ID_h) \\ F_2 = \min(IM_h) \end{cases} \tag{1}$$

$$\begin{cases} F_3 = \min(ID_{Q_{out}}) \\ F_4 = \min(IM_{Q_{out}}) \end{cases} \tag{2}$$

$$\begin{cases} F_5 = \min(ID_{Def}) \\ F_6 = \min(IM_{Def}) \end{cases} \tag{3}$$

Where,

$$ID_h = \frac{\max_{sn}\left[\max_n\left(h_n^{sn}\right)\right] - \min_{sn}\left[\min_n\left(h_n^{sn}\right)\right]}{2} \tag{4}$$

$$IM_h = \frac{\max_{sn}\left[\max_n\left(h_n^{sn}\right)\right] + \min_{sn}\left[\min_n\left(h_n^{sn}\right)\right]}{2} \tag{5}$$

$$ID_{Q_{out}} = \frac{\max_{sn}\left[\max_n\left(Q_{out,n}^{sn}\right)\right] - \min_{sn}\left[\min_n\left(Q_{out,n}^{sn}\right)\right]}{2} \tag{6}$$

$$IM_{Q_{out}} = \frac{\max_{sn}\left[\max_n\left(Q_{out,n}^{sn}\right)\right] + \min_{sn}\left[\min_n\left(Q_{out,n}^{sn}\right)\right]}{2} \tag{7}$$

$$ID_{Def} = \frac{\max_{sn}\left[Def_{sn}\right] - \min_{sn}\left[Def_{sn}\right]}{2} \tag{8}$$

$$IM_{Def} = \frac{\max_{sn}\left[Def_{sn}\right] + \min_{sn}\left[Def_{sn}\right]}{2} \tag{9}$$

Where:

ID_h : The interval deviation for the water depth (m),

IM_h : The interval average for the water depth (m),

$ID_{Q_{out}}$: The interval deviation for the outflow discharge (m^3/s),

$IM_{Q_{out}}$: The interval average for the outflow discharge (m^3/s),

ID_{Def} : The interval deviation for the water demand deficit (m^3/s),

IM_{Def} : The interval average for the water demand deficit (m^3/s),

sn : The flood scenario,

h_n^{sn}: The water head in the n th flood routing step for the sn th scenario (m),

$Q_{out,n}^{sn}$: The outflow discharge in the n th flood routing step for the sn th scenario (m^3/s),

Def_{sn}: The water demand deficit for the sn th scenario (m^3/s),

The h_n^{sn} was calculated from Eqs. (10) and (11) as a function of chosen outlet/weir (OW_{type}), the time step for routing (t_n), and inflow flood discharge at n th time step for the selected inflow hydrograph INF [$I_{INF}(t_n)$].

$$h_n^{sn} = fun_1\left[I_{INF}(t_n), t_n, OW_{type}\right] \tag{10}$$

$$Q_{out,n}^{sn} = fun_2\left[I_{INF}(t_n), t_n, OW_{type}\right] \tag{11}$$

Finally, Def_n^{sn} was computed using Eq. (12).

$$Def_{sn} = \frac{WD_T - \sum_{n=0}^{To} Q_{out,n}^{sn}}{WD_T} \tag{12}$$

Where:

WD_T: Total water demand during the flood occurrence.

2.2.3.2 Cost-based objective functions

The seventh objective function for this optimization model was minimizing the selected orifice/weir characteristics, defined by Eq. (13), to optimize the cost required for constructing the orifice/weir.

$$F_7 = \min(OW_C) \tag{13}$$

Where:

OW_C: The orifice/weir characteristics to be optimized were cross-sectional area (A_O) for the orifice, weir's angle (θ_T) of the triangular weir, base distance for the proportional weir (s), and the weir width of the rectangular weir (L_R).

2.2.4 Constraints

The primary constraint for the proposed optimization framework in water balance constraint through numerical analysis of the reservoir routing equation [Eq. (14)] (Liu et al. 2017). Another constraint could be considered in terms of flood discharge capacity [Eq. (15)]. Finally, the reservoir storage volume should be limited by Eq. (16) (Liu et al. 2017).

$$\frac{dS_t}{dt} = I(t) - Q_{out}(t) \tag{14}$$

$$Q_{out} < \min\left[Q_{\max}(h_t), Q_{\max}^{down}\right] \tag{15}$$

$$S_l \le S_t \le S_u \tag{16}$$

Where:

$I(t)$: The reservoir inflow (m^3/s),

S_t: The reservoir storage (m^3/s),

$Q_{out} < Q_{\max}(h_t)$: The orifice/weir,

$Q_{\max}(h_t)$: The maximum discharge capacity of the reservoir for the water level of h_t (m^3/s),

$Q_{\max}^{down}$: The safe discharge for flood control in downstream (m^3/s),

S_l: The minimum reservoir storage (m^3),

S_u: The maximum reservoir storage (m^3).

2.3 Multi-criteria decision-making (MCDM) model

In this study, a robust MCDM method, the so-called complex proportional assessment (COPRAS) technique, was utilized to rank the options resulting from the optimization model. Considering the above definition, the most superior alternative was the option related to the most significant ranking. Hence, the MCDM model resulted in a tranfromation of several criteria values into a single final assessment to be used for assessing, ranking, and selecting the best superior alternatives (Zhu et al. 2018) discussed in the Supplementary materials, section S4. Applying the COPRAS method to obtain the superior alternative comprises six main steps, as noted in Supplementary materials, section S5 (Pitchipoo et al. 2014).

3 Results

The proposed innovative framework developed a hybrid multi-criteria decision-making- multi-objective particle swarm optimization (MCDM-MOPSO) model, which endeavored to minimize the averages and radii of water demand deficit, flood damage, and flood overtopping, and outlets characteristics as the cross-sectional area for the orifice, weir's angle for the triangular weir, weir's width for the rectangular weir, and base distance for the proportional weir as well as ranking the optimum solutions to obtain the most appropriate optimum design.

3.1 The MOPSO model results

3.1.1 Problem definition

The proposed framework was applied to an extended version of an example adopted from Paik (2008) to prove the efficiency and advantage of the presented methodology. In this example, four same prismatic reservoirs with 12 km^2 surface areas were assumed to be customized to four outlet types: triangular, proportional, and rectangular weirs and orifice. Then, fifty inflow hydrographs based on five patterns of flood pulse, triangular, broad peak, abrupt wave, and double-peak were hypothesized, as shown in Fig. 2. These inflow hydrographs occurred within the time of $t_0 = 0$ (s) to $t_n = 8000$ (s) with 200 -second-time steps. Furthermore, the lower and upper bounds of decision variables for different outlet types were written in Table S.1, Supplementary materials, section S7. In addition, the modified Euler was utilized as the numerical tool for solving the governing equation. Finally, Earth's gravity was set to be 9.81 m/s^2 , and the time step for the numerical analysis was 200 seconds.

3.1.2 Optimal outlets solutions

Using 50 inflow flood scenarios, the proposed MOPSO model defined optimum geometrical characteristics of the reservoirs with different outlet specifications. Therefore, 30 Pareto-optimal solutions were shown in Fig. 3 for the orifice, and 20 Pareto-optimal answers were indicated in the same figure for optimum outlets characteristics of other outlet types, wherein the values obtained for the Pareto-optimal solutions were noted in Supplementary material, section S8, Tables S.2 to S.5.

Fig. 3 showed the resulted values for the outflow, deficit of water, and head of water in the Pareto-optimal solutions. The results revealed that the MOPSO optimization algorithm selected characteristics associated with specific objective values. It showed that the optimal values for the IM_h were in the range of 0.011742 to 0.013689 (m) for the orifice, 0.383572 to 4.61888 (m) for the proportional weir, 0.502686 to 1.254345 (m) for the rectangular weir, and 0.28783 to 0.336561 (m) corresponding to the triangular weir. In addition, the optimum values for the $IM_{Q_{out}}$ were in the range of 0.106784 to 2.74204 (m^3/s) for the orifice, 1.424646 to 10.23736 (m^3/s) for the proportional weir, 5.95493 to 10.24508 (m^3/s) for the rectangular weir, and 0.188633 to 1.420806 (m^3/s) for the triangular weir. Finally, the optimal values of the IM_{Def} were in the range of 7.688% to 27.799% for the orifice, 0.5562% to 1.6672% for the proportional weir, and 0.0901% to 0.3831% corresponding to the triangular weir, and 0.9404% to 1.6735% for the rectangular weir.

Fig. 4 indicated a comparison between the outflow discharges from different outlet types. This figure illustrated that the triangular weir was the safest outlet to limit the flood damage since it provided a minor discharge. After that, the safest one was the orifice and proportional weir.

Finally, it was notable that the rectangular weir was the most disastrous outlet type concerning flood damage due to the highest outlet discharge.

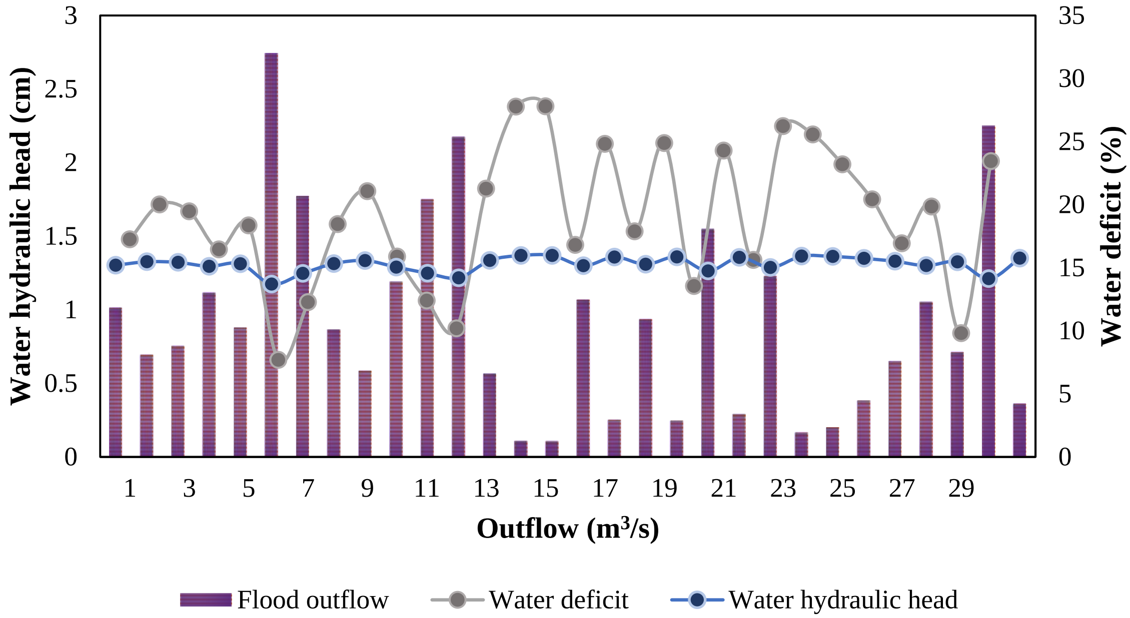

(a)

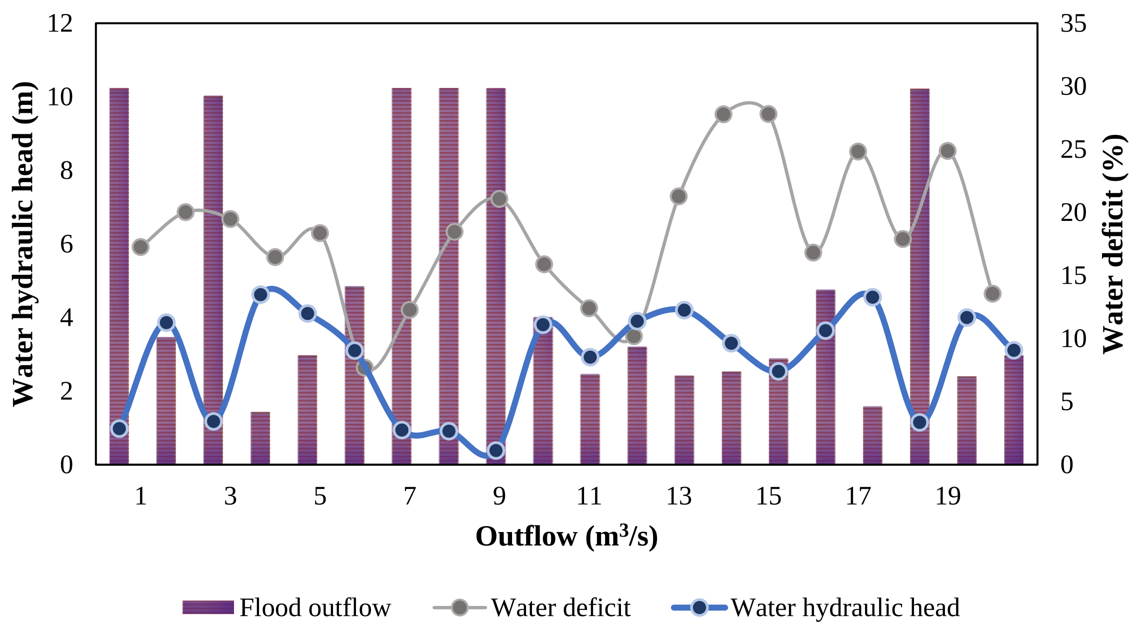

(b)

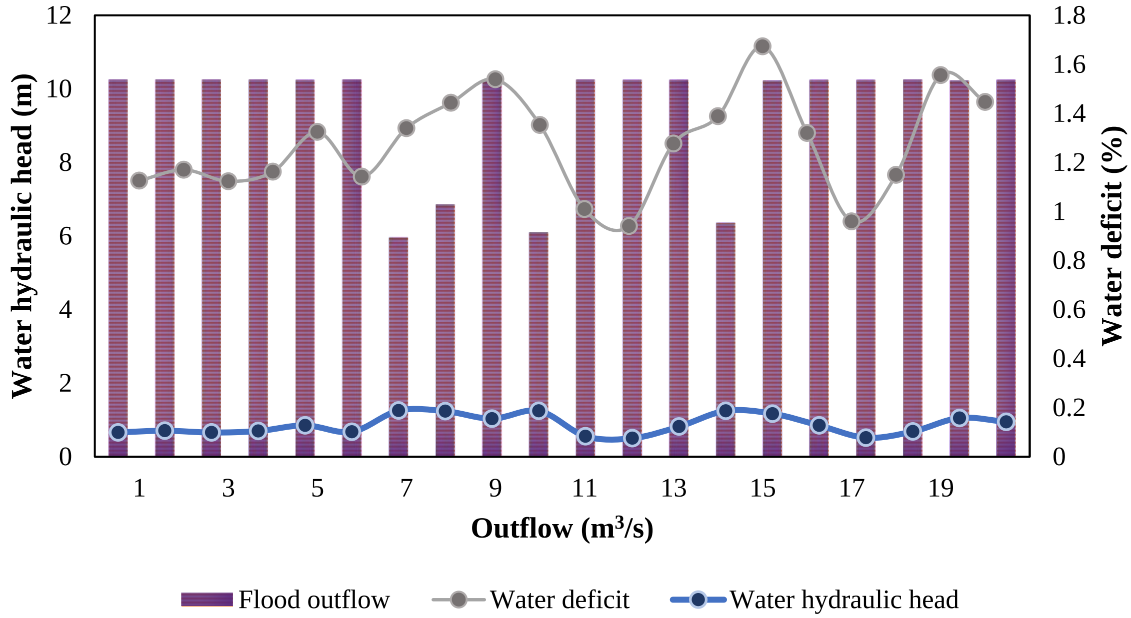

(c)

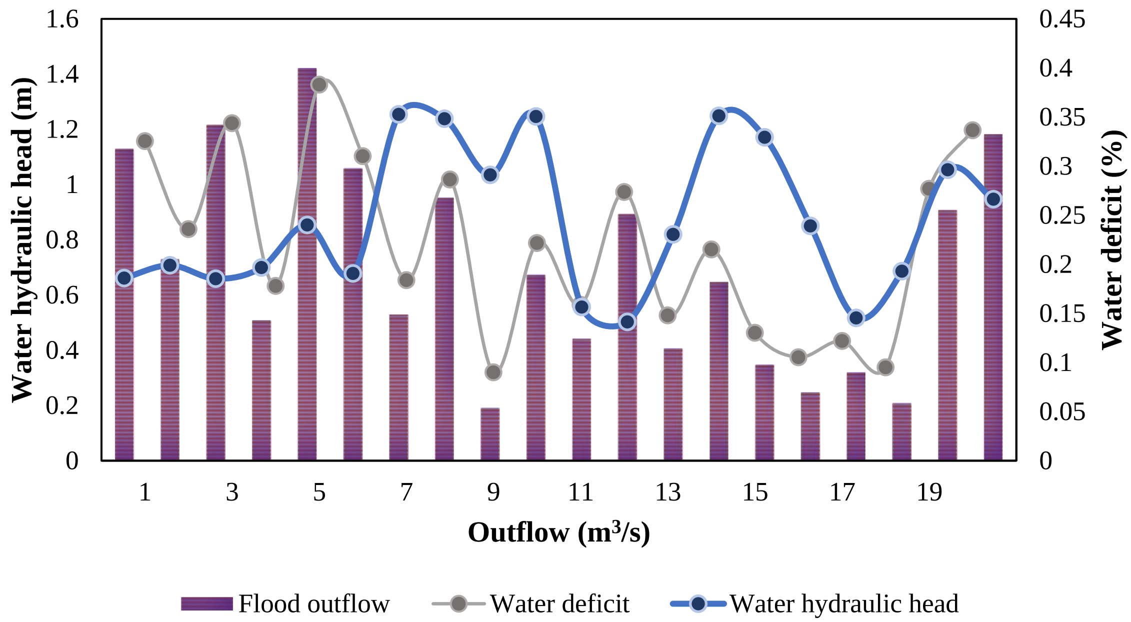

(d)

Fig. 3 Pareto-optimal solutions of the MOPSO model for outlets of a) Orifice, b) Proportional, c) Rectangular, and d) Triangular weirs

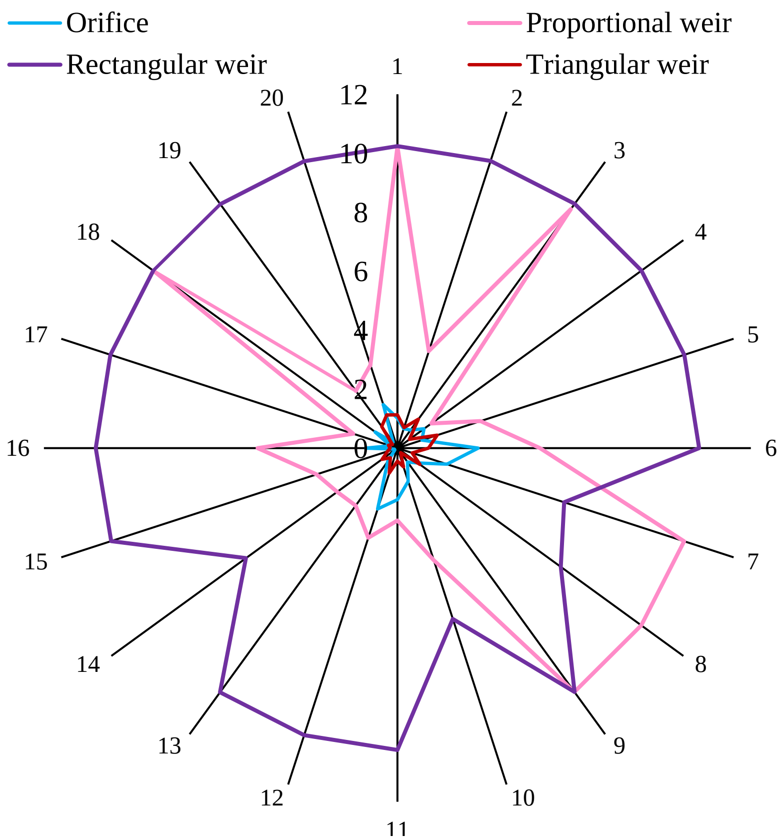

Fig. 4 The outflow discharges comparison for different outlet types

3.2 The MCDM model results

3.2.1 Entropy Shannon method results

The Entropy Shannon technique was implemented to obtain the importance weights of different objectives using the decision matrices consisting of the Pareto-optimal solutions for different outlet types, which were in the dimensions of 30×7 for the orifice and 20×7 for other outlet types. Table S.6 illustrated the indices acquired by applying this technique in Supplementary materials, section S9.

3.2.2 The COPRAS approach results

Figs. 5 showed the utilities obtained from the COPRAS model to rank Pareto-optimal solutions. As this figure showed, all alternatives' utilities were almost more than 0.5, which showed the suitability of all solutions. The detailed procedure was shown in the Supplementary materials, section S10.

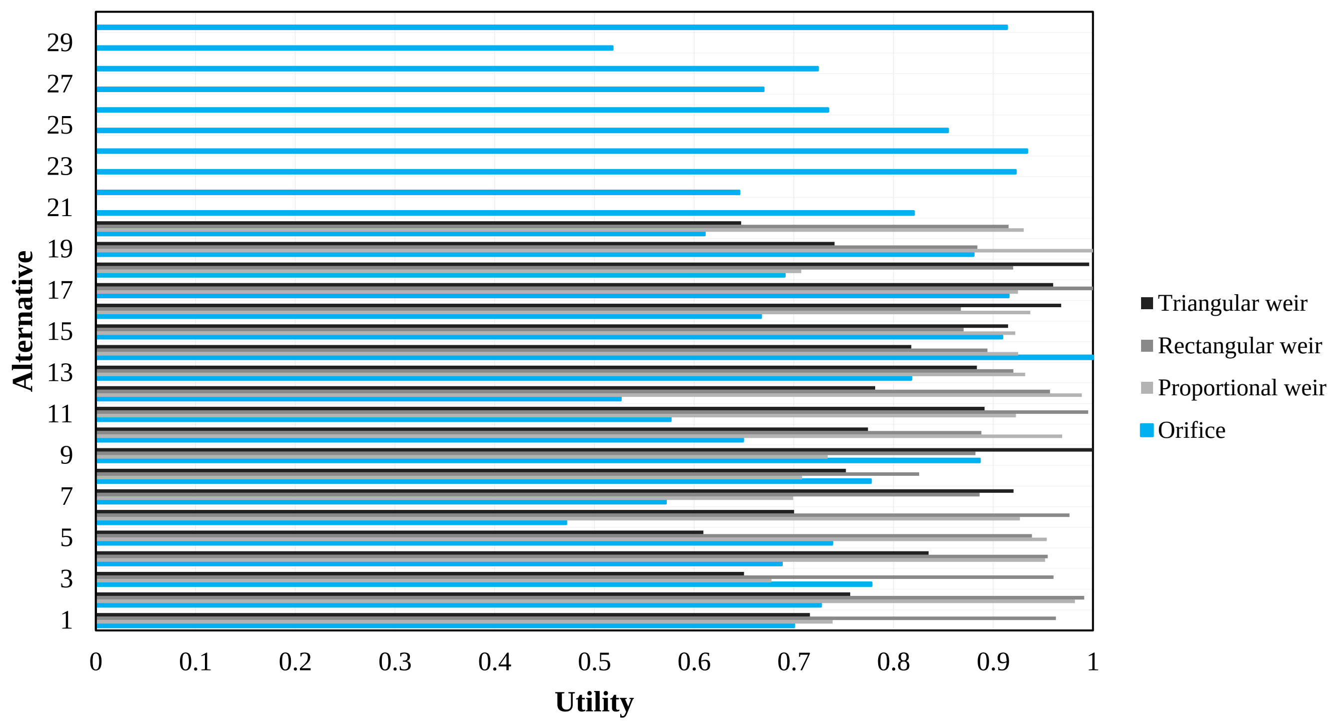

Fig. 5 The COPRAS utilities for ranking Pareto-optimal solutions outlet types of the orifice and proportional, rectangular, and triangular weirs

3.3 The MCDM-MOPSO model optimal design

Table 1 indicated the selected optimal design for different outlet types after applying the COPRAS MCDM model to the results of the MOPSO model. This table showed that the values of optimum decision variables for the best Pareto-optimal solutions were selected as the superior optimum design.

Table 1 The hybrid MCDM-MOPSO model optimal design

Outlet type	Design parameters	
	Coefficient	**Geometry**
Orifice	Coefficient (C_O): 0.582183 Correction factor (λ_O): 0.2	Cross-sectional area (A_O): 2
Triangular weir	Coefficient (C_T): 0.2	Weir's angle (θ_T): 51.66777°
Rectangular weir	Coefficient (C_R): 0.8	Width (L_R): 6.59681
Proportional weir	Coefficient (C_P): 0.463109	Base distance (s): 2

4 Discussion

The presented MCDM-MOPSO model could efficiently provide the optimal designs for the reservoirs and outlets while meeting the water demand requirements. The following sections provided a detailed discussion of the proposed model's results.

4.1 The MOPSO model discussion

Fig. 3 indicated the Pareto-optimal solutions for each outlet type from the MOPSO optimization model. This figure illustrated that the average value of the water depth had the highest maximum amount for the proportional weir and the lowest amount for the orifice; Furthermore, the variations in the average depth were highest for the proportional weir and the lowest for the orifice. This showed that when the water depth behind the reservoir was a significant concern for the designer, it would be better to construct the orifice as the flood outlet control.

Then, the maximum values for the average outflow discharge were the highest for the orifice and the proportional weir, while the minimum amounts of this parameter were the lowest for the orifice. Moreover, the range of the outflow discharge for the proportional weir was more than other outlet types, and for the triangular weir was less than others. This illustrated that in conditions with a limitation for the range of outflow from the reservoir outlet, it would be better to build a triangular weir downstream of the reservoir as a conservative selection.

Finally, the maximum values of the average water deficit for the orifice were the highest, and the triangular weir was the lowest among different outlet types. In the meantime, the range of water deficit for the triangular weir was the lowest compared to other outlet types. In addition, Fig. 6 showed the results of water deficit demand from the proposed model and the previously presented model by Nematollahi et al. (2022) on the same problem based on the hybrid non-dominated sorting genetic algorithm- III (NSGA-III) and graph model for conflict resolution (GMCR). This figure illustrated that the proposed model could substantially decrease the water deficit demand, proving the proposed model's efficiency and novelty.

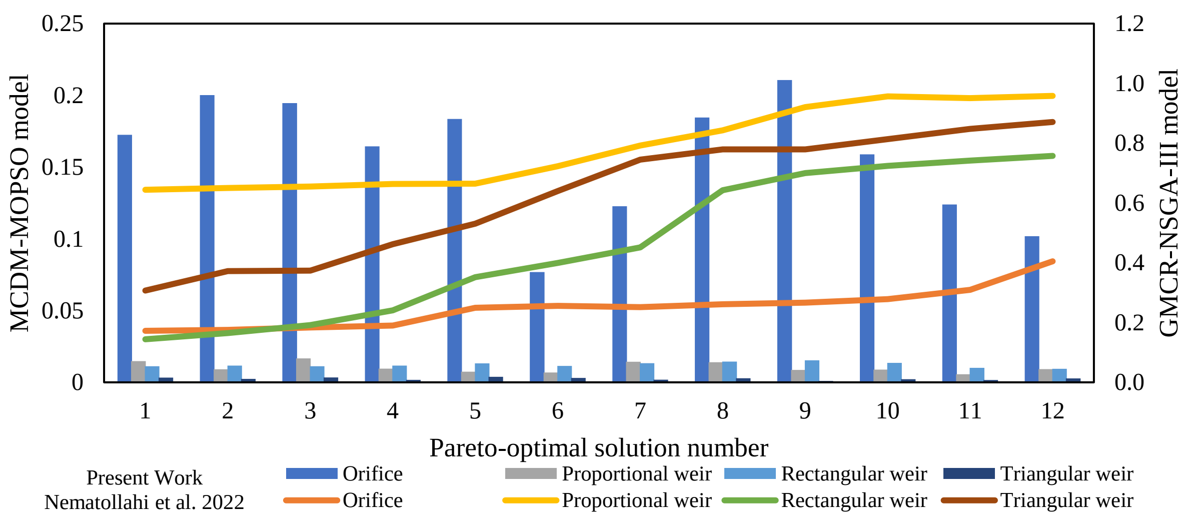

Fig. 6 Comparison of the downstream water deficit based on the proposed MCDM-MOPSO model and the GMCR-NSGA-III model by Nematollahi et al. (2022)

4.2 The MCDM model discussion

4.2.1 Entropy Shannon method

As shown in Table S.6, Supplementary materials, section S9, the objectives of the MOPSO model had almost similar weights. This revealed that the importance of different objectives used within the optimization model was not far from each other. Therefore, these importance weights assigned to the objectives (criteria) were utilized within the MCDM model to find the COPRAS decision-making results to determine the most appropriate and superior optimal design.

4.2.2 The COPRAS method

Figs. 7 indicated the Box plot for the utilities of different outlet types from the COPRAS model. This figure indicated that the utilities of the optimal solutions for the rectangular weir were in the more appropriate ranges than other outlet types, which showed that the proposed optimal solution worked more suitably with this outlet type rather than others. On the other hand, although the utility values for the orifice had suitable values, they were less than other outlet types.

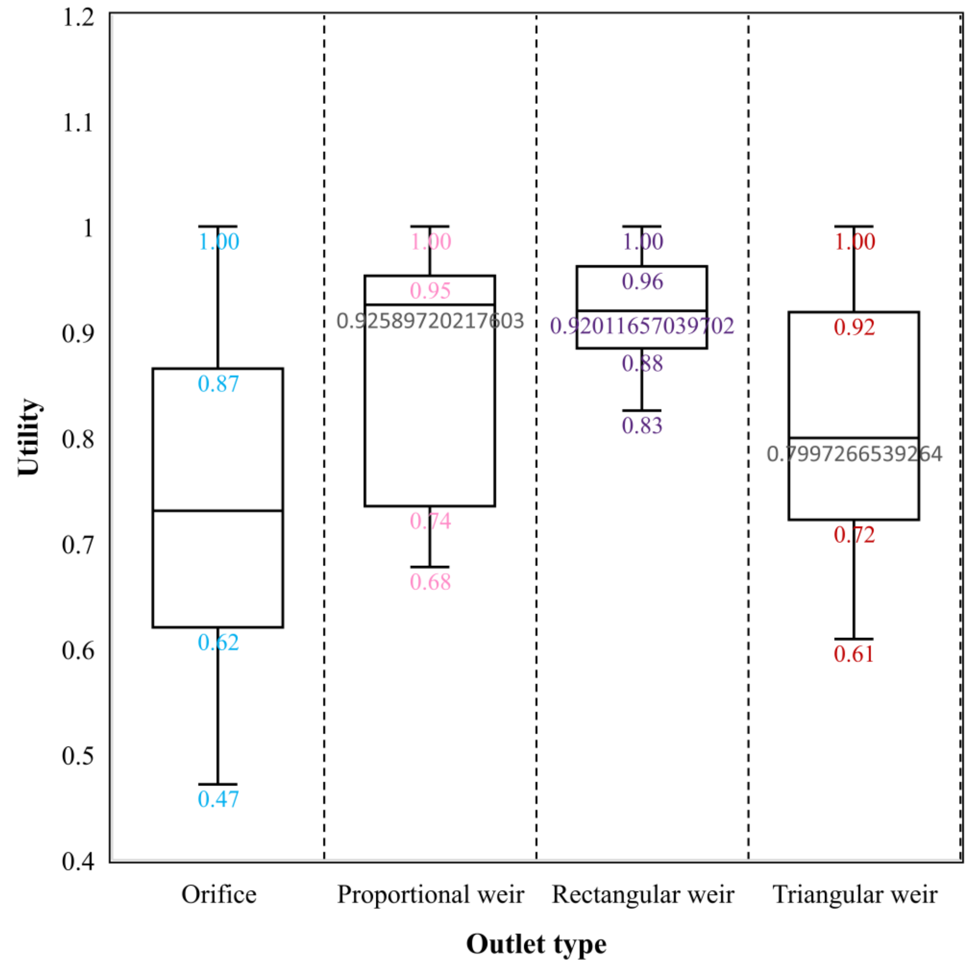

Fig. 7 Box plot of utilities for different outlet types

4.3 The MCDM-MOPSO model discussion

As Table 1 shown, the proposed COPRAS-MOPSO model could design the reservoirs with different outlet types efficiently. Finally, it could be concluded that the presented model could be used beneficially by the designers after applying it to specific problem specifications during the flood.

5 Conclusion

This study proposed a novel hybrid multi-criteria decision-making- multi-objective particle swarm optimization (MCDM-MOPSO) model to define the most suitable optimum characteristics of the reservoirs concerning four types of outlets as triangular, proportional, and rectangular weirs and orifice by minimizing the averages and radii of flood overtopping, downstream flood damage, and water demand deficit using the non-linear interval number programming (NINP) technique and outlets characteristics. The input to this framework consisted of fifty inflow hydrographs based on five common patterns to cover almost all inflow types: triangular, flood pulse, broad peak, abrupt wave, and double-peak. The equations for flood routing were solved using a well-known scheme of a commonly-used numerical method, modified Euler's method during the optimization procedure. Applying the inflow flood scenarios within the MOPSO model using the above-mentioned numerical method resulted in a series of Pareto-optimal solutions. Finally, the most appropriate optimum design for the reservoirs and their outlets was selected among the Pareto-optimal solutions using the complex proportional assessment (COPRAS) method based on the importance weights obtained by the Entropy Shannon technique. Applying the proposed hybrid MCDM-MOPSO model to an example proved this methodology's efficiency and practicality. Furthermore, it illustrated that the triangular weir was the safest outlet for flood conditions, while the rectangular weir was the most hazardous outlet considering flood damage.

Authors' contributions All authors contributed to the study's conception and design. Conceptualization, methodology, software, investigation, and review and editing were performed by B. Nematollahi, M. R. Nikoo, A. H. Gandomi, N. Talebbeydokhti, and G. R. Rakhshandehroo.

The first draft of the manuscript was written by B. Nematollahi, and all authors reviewed and edited previous versions and approved the final manuscript.

Funding The authors declare that no funds, grants, or other support were received during the preparation of this manuscript.

Data Availability Not applicable.

Code Availability Not applicable.

Declarations

Ethical approval All authors approved ethical standards and consented to participate in and publish this manuscript.

Consent to participate Not applicable.

Consent to Publish Not applicable.

Conflict of interest The authors declare that they have no known competing financial interests or personal relationships that could have appeared to influence the work reported in this paper.

6 References

Alipour MH (2015) Risk-informed decision making framework for operating a multi-purpose hydropower reservoir during flooding and high inflow events, case study: Cheakamus River System. Water Resources Management 29(3). https://doi.org/10.1007/s11269-014-0844-3.

Ashrafi S, Kerachian R, Pourmoghim P, Behboudian M, Motlaghzadeh K (2022) Evaluating and improving the sustainability of ecosystem services in river basins under climate change. Science of the Total Environment 806(3):150702. https://doi.org/10.1016/j.scitotenv.2021.150702.

Badfar M, Barati R, Dogan E, Tayfur G (2021) Reverse flood routing in rivers using linear and non-linear Muskingum models. Journal of Hydrologic Engineering 26(6):04021018.

Brito M, Evers M (2016) Multi-criteria decision-making for flood risk management: a survey of the current state of the art. Natural Hazards and Earth System Sciences 16:1019-1033. https://doi.org/10.519/nhess-16-1019-2016-supplement.

Chen S, Hou Z (2004) Multicriterion decision making for flood control operations: theory and applications. Journal of the American Water Resources Association 40(1):67-76. https://doi.org/10.1111/j.1752-1688-2004-tb01010.x.

Chen H, Wang W, Chen X, Qiu L (2020) Multi-objective reservoir operation using particle swarm optimization with adaptive random inertia weights. Water Science and Engineering 13(2):136-144. https://doi.org/10.1016/j.wse.2020.06.005.

Durbach IN, Stewart TJ (2012) Modeling uncertainty in multi-criteria decision analysis. Eur. J. Oper. Res. 223(1):1-14, https://doi.org/10.1016/j.ejor.2012.04.038.

Eldardiry H, Hossain F (2021) The value of long-term streamflow forecasts in adaptive reservoir operation: The case of the High Aswan Dam in the Transboundary Nile river basin. Journal of Hydrometeorology 22(5):1099-1115.

Fu G (2008) A fuzzy optimization method for multi-criteria decision making: an application to reservoir flood control operation. Expert Systems with Applications 34(1):145-149. https://doi.org/10.1016/j.eswa.2006.08.021.

Gang X (2005) Application of ant colony algorithm to reservoir optimal operation. Advances in Water Science.

Gioia A (2016) Reservoir routing on double peak design flood. Water 8(12):553.

Hui, R. Flood storage allocation rules for parallel reservoirs, *Thesis for master of science*, University of California, Davis, Approved by Lund, J.R., Younis, B., and Sandoval Solis, S., 2013.

Jacob ACP, Rezende OM, de Sousa MM, de França Ribeiro LB, de Oliveira AKB, Arrais CM, Miguez MG (2019) Use of detention basin for flood mitigation and urban requalification in Mesquita, Brazil. Water Science and Technology 79(11):2135-2144.

Jiang C, Han X, Liu GR, Liu GP (2008) A non-linear interval number programming method for uncertain optimization problems. European Journal of Operational Research 188(1):1-13.

Jothiprakash V, Arunkumar R (2013) Optimization of hydropower reservoir using evolutionary algorithms coupled with chaos. Water Resour. Manag. 27(7):1963-1979, https://doi.org/10.1007/s11269-013-0265-8.

Karaboga D, Bagis A, Haktanir T (2004) Fuzzy logic based operation of spillway gates of reservoirs during floods. J Hydrol. Eng. 9(6):544-549.

Karaboga D, Bagis A, Haktanir T (2008) Controlling spillway gates of dams by using fuzzy logic controller with optimum rule number. Appl. Soft Comput. 8(1):232-238.

Liu X, Chen L, Zhu Y, Singh VP, Qu G, Guo X (2017) Multi-objective reservoir operation during flood season considering spillway optimization. Journal of Hydrology. https://doi.org/10.1016/j.jhydrol.2017.06.044.

Malekmohammadi B, Zahraei B, Kerachian R (2011) Ranking solutions of multi-objective reservoir operation optimization models using multi-criteria decision analysis. Expert Syst. Appl. 38(6):7851-7863.

Mamun A, Shawwash Z, Abdalla A, Li J, Siu T (2015) Application of a goal programming algorithm to incorporate environmental requirements in a multi-objective Columbia River Treaty Reservoir optimization model. Canadian Water Resources Journal 40(1):111-125, 2015, https://doi.org/10.1080/07011784.2014.985514.

Nematollahi B, Hashempour Bakhtiari P, Talebbeydokhti N, Rakhshandehroo GR, Nikoo MR, Gandomi AH (2022) A stochastic conflict resolution optimization model for flood management in detention basins: Application of fuzzy graph model. Water 14(5):774, https://doi.org/10.3390/w14050774.

Nematollahi B, Niazkar M, Talebbeydokhti N (2021) Analytical and numerical solutions to level pool routing equations for simplified shapes of inflow hydrographs. Iran J Sci. Technol. Trans. of Civ. Eng. https://doi.org/10.1007/s40996-021-00757-x.

Paik K (2008) Analytical derivation of reservoir routing and hydrological risk evaluation of detention basins. Journal of Hydrology 352(1-2):191-201.

Pitchipoo P, Vincent D, Rajini N, Rajakarunakaran S (2014) COPRAS decision model to optimize blind spot in heavy vehicles: a comparative perspective. Procedia Engineering 97:1049-1059. https://doi.org/10.1016/j.proeng.2014.12.383.

Pourshahabi S, Rakhshandehroo G, Talebbeydokhti N, Nikoo MR, Masoumi F (2020) Handling uncertainty in optimal design of reservoir water quality monitoring systems. Environmental Pollution 266:115211.

Roozbahani A, Ghased H, Hashemy Shahedany M (2021) Inter-basin water transfer planning with grey COPRAS and fuzzy COPRAS techniques: A case study in Iranian Central Plateau. Science of the Total Environment 726:138499. https://doi.org/10.1016/j.scitotenv.2021.138499.

Shuai W, Huang Xiaomin LX (2012) Multi-objective optimization of reservoir flood dispatch based on MOPSO algorithm. *In* 2012 8th International Conference on Natural Computation (ICNC 2012).

Sin-Lau H, Shiyou Y, Guangzheng N, Edward L, Ho-ching Chris W (2005) A particle swarm optimization-based method for multi-objective design optimizations. IEEE Transactions on Magnetics 41(5):1756-1759.

Su HT, Tung YK (2014) Multi-criteria decision making under uncertainty for flood mitigation. Stoch. Env. Res. Risk A28(7):1657-1670, https://doi.org/10.1007/s00477-013-0818-7.

Wang XJ, Zhao RH, and Hao YW (2011) Flood control operations based on the theory of variable fuzzy sets. Water Resour. Manage. 25(3):777-792.

Yazdandoost F, Razavi H, Izadi A (2021) Optimization of agricultural patterns based on virtual water considerations through integrated water resources management modeling. International Journal of River Basin Management 1-22. https://doi.org/10.1080/15715124.2021.1879093.

Yu YB, Wang BD, Wang GL, Li W (2004) Multi-person multi-objective fuzzy decision-making model for reservoir flood control operation. Water Resour. Manage. 18(2):111-124.

Zhu F, Zhong P, Xu B, Wu Y, Zhang Y (2016) A multi-criteria decision-making model dealing with correlation among criteria for reservoir flood control operation. Journal of Hydroinformatics 18(3). https://doi.org/10.2166.hydro.2015.055.

Zhu F, Zhong P, Sun Y (2018) Multi-criteria group decision making under uncertainty: Application in reservoir flood control operation. Environmental Modelling and Software 100:236-251, https://doi.org/10.1016/j.envsoft.2017.11.032.

Supplementary Materials

A Multi-Criteria Decision-Making Optimization Model for Flood Management in Reservoirs

1st Author

Banafsheh Nematollahi

Ph.D., Department of Civil and Environmental Engineering, Shiraz University, Shiraz, Iran. Email Address: b.Nematollahi@shirazu.ac.ir

2nd Author (Corresponding Author)

Mohammad Reza Nikoo

Associate Professor, Department of Civil and Architectural Engineering, Sultan Qaboos University, Muscat, Oman. Email Address: m.reza@squ.edu.om

3rd Author

Amir H. Gandomi

Professor, Faculty of Engineering and Information Technology, University of Technology Sydney, Ultimo, Australia. Email Address: gandomi@uts.edu.au

4th Author

Nasser Talebbeydokhti

Professor, Department of Civil and Environmental Engineering, Head of Environmental Research and Sustainable Development Center, Shiraz University, Shiraz, Iran. Email Address: taleb@shirazu.ac.ir

5th Author

Gholam Reza Rakhshandehroo

Professor, Department of Civil and Environmental Engineering, Shiraz University, Shiraz, Iran. Email Address: rakhshan@shirazu.ac.ir

S1 Outlet formulation

The outlets' formulations for the orifice and triangular, rectangular, and proportional weirs were provided in the following, respectively.

$$Q_{out} = \lambda_O C_O A_O \sqrt{2gh} \tag{S.1}$$

$$Q_{out} = \frac{8}{15} C_T \sqrt{2gh^5} \tan\left(\frac{\theta_T}{2}\right) \tag{S.2}$$

$$Q_{out} = \frac{2}{3} C_R L_R \sqrt{2gh^3} \tag{S.3}$$

$$Q_{out} = C_P \left(h + \frac{2}{3} s\right) \tag{S.4}$$

$$\frac{x_P(y_P)}{b_P} = 2\left[\frac{2}{\pi} \arctan\left(\sqrt{\frac{y_P}{s}}\right)\right] \tag{S.5}$$

Where:

Q_{out} : Outflow from the outlet/weirs (m^3/s),

h : Water depth in the reservoir (m),

λ_O : Orifice formula correction factor,

C_O : Orifice coefficient,

A_O : Orifice cross-sectional area (m^2),

C_T : The coefficient of the triangular weir,

θ_T : Triangular weir's angle (degrees),

C_R : Rectangular weir coefficient,

L_R : Rectangular weir width (m),

C_P : Proportional weir coefficient,

s : Proportional weir base distance (m),

x_P : Proportional weir width at the water surface (m),

y_P : Vertical elevation of the water depth for the proportional weir (m),

b_P : Proportional weir constant,

g : Gravitational acceleration constant (m/s^2).

S2 Flood routing numerical analysis

The numerical analysis for the flood routing equation was performed using a robust scheme of the well-known numerical method, the Runge-Kutta method, as modified by Euler's approach (Badfar et al. 2021). In this method, the inflow and outlet outflow for the specific inflow hydrograph INF were defined by Eqs. (S.6) and (S.7), respectively.

$$\left(I_{INF}\right)_{1,n} = f_{INF}(t_n) \tag{S.6}$$

$$\left(Q_{out}\right)_{1,n} = f_{out}(h_n) \tag{S.7}$$

Where:

$(I_{INF})_{1,n}$: First approximation of inflow at the n^{th} flood routing step (m^3/s),

t_n: Flood routing step (s),

$(Q_{out})_{1,n}$: First approximation of outflow from the orifice/weirs at the n^{th} flood routing step (m^3/s),

h_n: Water hydraulic depth in the reservoir at the n^{th} flood routing step (m),

Then, the first numerical coefficient ($k_{1,n}$) was calculated for the total flooding time (T_{tot}) after specifying the reservoir area ($Area$) and time step (dt).

$$k_{1,n} = \left(\frac{dt}{Area}\right)\left[(I_{INF})_{1,n} - (Q_{out})_{1,n}\right]; n = 0,1,\ldots,T_{tot} \tag{S.8}$$

Next, the second series of inflow and outflow values were approximated using the first numerical coefficient and the time step as Eqs. (S.9) and (S.10).

$$(I_{INF})_{2,n} = f_{INF}(t_n + 0.5\times dt) \tag{S.9}$$

$$(Q_{out})_{2,n} = f_{out}(h_n + 0.5\times k_{1,n}) \tag{S.10}$$

Using the results of the above equations, the second numerical coefficient ($k_{2,n}$) was calculated by Eq. (S.11).

$$k_{2,n} = \left(\frac{dt}{Area}\right)\left[(I_{INF})_{2,n} - (Q_{out})_{2,n}\right]; n = 0,1,\ldots,T_{tot} \tag{S.11}$$

Finally, the time and hydraulic height values for the next step were calculated from Eqs. (S.12) and (S.13).

$$h_{n+1} = h_n + k_{2,n} \quad \text{(S.12)}$$

$$t_{n+1} = t_n + dt \quad \text{(S.13)}$$

S3 Implementation steps for multi-objective particle swarm optimization (MOPSO) optimization algorithm

The particle swarm optimization (PSO) approach is a commendable intelligent optimization technique introduced by Kennedy and Eberhart (1995) based on the birds' predatory reactions. In this approach, each possible solution for the optimization model is considered a "particle" in a searching system that can change its position within the solutions system to increase the value of the fitness function until the birds obtain the optimum position. The speed and dynamic location of the particles are defined using two extreme values: 1. The optimum solution for the particle is acquired within the evolutionary procedure (individual extreme value- *pBest*), and 2. The optimum solution is considered the entire population within the evolutionary process (global extreme value- *gBest*), so the PSO can be applied to an optimization problem by identifying the particles' global and individual extreme values. It has been proved that the PSO approach has a very intense priority for complex optimization problems compared to the conventionally-used optimization approaches since: 1. There is no significant requirement for the optimization objectives within the process; 2. The optimization algorithm has a fast and acceptable convergence because of the fitness based on the probability evolution; and 3. There is a low probability of localized optimization because of the random search space (Shuai and Huang Xiaomin 2012).

The following steps should be followed to implement the MOPSO algorithm into the reservoir optimization problem, as shown in Fig. S.1.

1. The first step creates the internal particle swarm and external set. For this purpose, first, the particles' optimum positions are created as *pBest* and *gBest* based on the fitness values of multiple objectives associated with each particle considering the zero for the initial velocities [$V(M)$] of the particles and Eq. (S.14) for calculating the population. Then, the external archives set is generated as *ExtArchive* with the scale of *SAr*, the maximum iteration times are set as *ItMax*, and the initial iteration time is set as zero (*It=0*).

$$Pop(M) = \underset{\min}{Range}(M) + R_1 \times \left[\underset{\max}{Range}(M) - \underset{\min}{Range}(M) \right] \tag{S.14}$$

Where:

$Pop(M)$: The population of the internal particle swarm with the scale of M,

$\underset{\min}{Range}(M)$: The minimum limit of the particle range,

$\underset{\max}{Range}(M)$: The maximum limit of the particle range,

R_1: A random number between zero and one.

2. In the second step, the non-dominated particles are chosen from the $Pop(M)$ to be copied in the *ExtArchive*. Then, the non-dominated particles are ordered in descending manner based on the crowded distance calculations considering the limitation of the numbers of the noninferior solutions to the *SAr*. Finally, the *gBest* are updated, and the elements of the Pareto fronts should guide particle swarm evolutions to the scattered areas of those elements.
3. The third step implements a variation operation for the internal particle swarm based on the updated internal particle swarm. First, the particle velocity and location are updated using Eqs. (S.15) and (S.16). Then, the range of the particle position should be checked to

be in the range of $\left[Pop_{\min}, Pop_{\max}\right]$. If the range of the particle is not within this limitation, the particle should be kept on the boundary, and the associated speed direction should be reversed as $-V_{up}(M)$. Finally, the mutation rate is calculated, and variation of the internal particle is applied when Eq. (S.17) is applicable.

$$V_{up}(M) = 0.4\left[V(M)\right] + R_1\left[PBest(M) - Pop(M)\right] + R_2\left[gBest(Ar) - Pop(M)\right] \quad \text{(S.15)}$$

$$Pop(M) = Pop(M) + V_{up}(M) \quad \text{(S.16)}$$

$$It < ItMax \times MuR \quad \text{(S.17)}$$

Where:

$V_{up}(M)$: The updated velocity with the scale of M,

$PBest(M)$: The optimal position in *pBest*,

$gBest(Ar)$: The optimal position in *ExtArchive*,

MuR: The mutation rate.

4. Finally, in the fourth step, the iteration times are investigated based on an updated version of *ExtArchive*. First, the fitness functions for multiple objectives associated with the mutant particle are calculated. Second, the non-dominated particles are moved to *ExtArchive,* and the *SAr* is rechecked to reduce the weak distributed elements. Finally, if the *ItMax* is exceeded, the procedure should be stopped, the *ExtArchive* is the final output, and the Pareto-optimal solution is obtained; otherwise, the process should be returned to step 2.

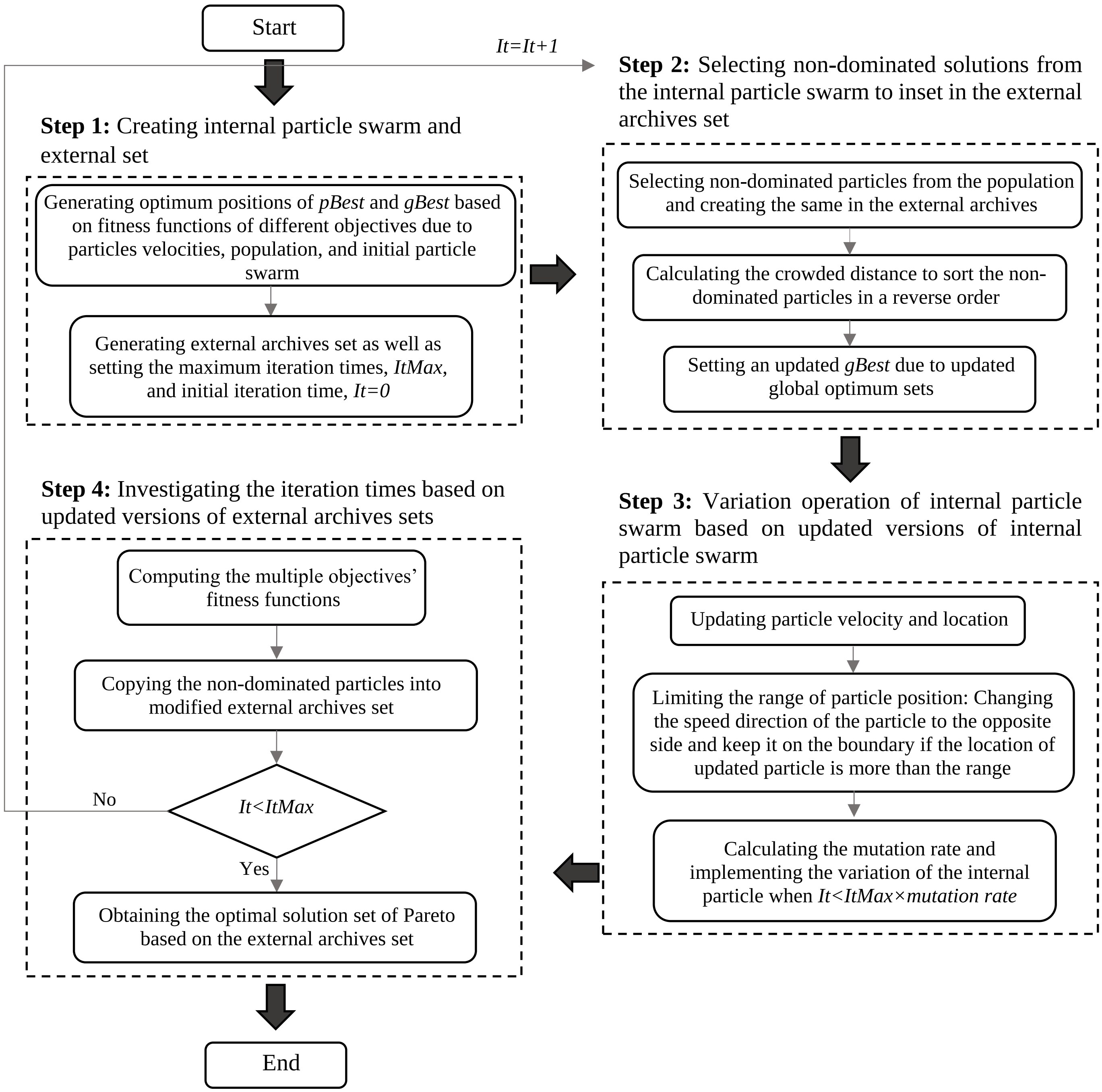

Fig. S.1 A schematic view of the MOPSO algorithm procedure

S4 Multi-criteria decision-making (MCDM) model

Each MCDM model can be formulated due to alternatives determination, criteria introduction, and weight quantifications. In this study, n alternatives resulted from the multi-objective optimization model and m criteria as the objectives of the optimization algorithm were assumed. The vectors of alternatives, weights, and criteria were $A=\{A_1,A_2,...,A_n\}$, $W=\{W_1,W_2,...,W_m\}$, and $C=\{C_1,C_2,...,C_m\}$, respectively. To this extent, the decision matrix could be calculated as $X=\left(x_{ij}\right)_{n\times m}$, in which x_{ij} was the result of evaluating the alternative A_i concerning criterion C_j where i and j represented the indices of the alternative and criterion, respectively. Then, the final assessment (M_i) evaluated the alternative A_i for all criteria to rank the options.

The Multi-criteria decision-making (MCDM) model consisted of four main steps (Fig. S.2). (1) Defining a series of alternatives to generate a decision matrix (X) and introducing the weights related to each criterion to prepare the weight matrix (W_C); (2) Formulating the MCDM model as a function of decision matrix and weight matrix [$F(X,W_C)$]; (3) Applying a deterministic measurement; and (4) Ranking alternatives based on the utilized MCDM model (Zhu et al. 2018). The alternatives adopted in each MCDM model could be determined explicitly and implicitly (Durbach and Stewart 2012).

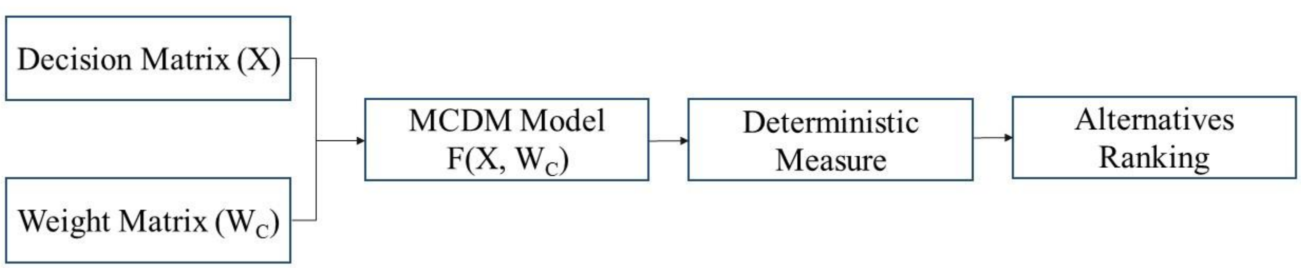

Fig. S.2 MCDM models procedure

S5 Complex proportional assessment (COPRAS) decision-making technique

The complex proportional assessment (COPRAS) technique is a commendable multiple-criteria decision-making (MCDM) method proposed by Zavadskas et al. (1994) to define the best superior option among several alternatives. This method considered the maximum and minimum criteria to include the desirable and undesirable effects separately. The process of applying the COPRAS method to obtain the most superior alternative comprises six main steps, as noted in the following (Pitchipoo et al. 2014).

1. In the first step, the vector of alternatives (A) and criteria (C) should be determined to define the decision matrix (X). In this study, the criteria were the values of the averages and radii of flood overtopping, peak outflow, and water deficit, and the alternatives were the results of the MOPSO optimization model. After that, the decision matrix was written as:

$$X = \begin{bmatrix} x_{11} & x_{12} & \cdots & x_{1m} \\ x_{21} & x_{22} & \cdots & x_{2m} \\ \vdots & \vdots & \ddots & \vdots \\ x_{n1} & x_{n2} & \cdots & x_{nm} \end{bmatrix} \tag{S.18}$$

   Where:

   n : The number of alternatives,

   m : The numbers of criteria.

   In this study, n and m were 60 and 6, respectively.

2. In the second step, the decision matrix (X) was normalized in each matrix's column concerning the most significant entry of that column to remove the effects of various unit measurements. The following equation was adopted to make the matrix X dimensionless.

$$x_{ij}^{\chi} = \frac{x_{ij}}{\sum_{i=1}^{n} x_{ij}}; i = 1, 2, ..., n; j = 1, 2, ..., m \tag{S.19}$$

$$X^{\chi} = \begin{bmatrix} x_{11}^{\chi} & x_{12}^{\chi} & \cdots & x_{1m}^{\chi} \\ x_{21}^{\chi} & x_{22}^{\chi} & \cdots & x_{2m}^{\chi} \\ \vdots & \vdots & \ddots & \vdots \\ x_{n1}^{\chi} & x_{n2}^{\chi} & \cdots & x_{nm}^{\chi} \end{bmatrix}$$

Where:

x_{ij}^{χ} : The decision matrix's dimensionless elements for alternative i and criterion j.

3. Third, the criteria weights should be clarified in the third step to identify the weighted dimensionless decision matrix ($\hat{X}^{\chi}$). The criteria weights were obtained from the Entropy Shannon method in this study. Then, the weighted scaleless decision matrix was calculated as follows:

$$\hat{X}^{\chi} = \begin{bmatrix} \hat{x}_{11}^{\chi} & \hat{x}_{12}^{\chi} & \cdots & \hat{x}_{1m}^{\chi} \\ \hat{x}_{21}^{\chi} & \hat{x}_{22}^{\chi} & \cdots & \hat{x}_{2m}^{\chi} \\ \vdots & \vdots & \ddots & \vdots \\ \hat{x}_{n1}^{\chi} & \hat{x}_{n2}^{\chi} & \cdots & \hat{x}_{nm}^{\chi} \end{bmatrix} \tag{S.20}$$

Where $\hat{x}_{ij}^{\chi} = x_{ij}^{\chi}.W_j$, in which W_j was the weight related to the criterion j.

4. In the fourth step, the desirable or maximizing index and undesirable or minimizing index were computed for each alternative. Finally, the maximizing indices were summed for an alternative i as R_{+i} and the minimizing indices were summed for an alternative i as R_{-i} in Eqs. (S.21) and (S.22).

$$R_{+i} = \sum_{j=1}^{k} \hat{x}_{ij}^{\chi} \tag{S.21}$$

$$R_{-i} = \sum_{j=k+1}^{m} \hat{x}_{ij}^{\chi} \tag{S.22}$$

Where:

k : The number of desirable criteria,

$m-k$: The number of undesirable criteria.

5. In the fifth step, the utilities related to different criteria were calculated from Eq. (S.23).

$$U_i = R_{+i} + \frac{\min_i R_{-i} \sum_{i=1}^{n} R_{-i}}{R_{-i} \sum_{i=1}^{n} \frac{\min_i R_{-i}}{R_{-i}}} \tag{S.23}$$

Where:

$\min_i R_{-i}$: The minimum of R_{-i} ,

U_i : The utility of the alternative i .

6. In the final step, the maximum value of the utilities was selected, and the final rank for each alternative was calculated as the following:

$$U_F = \max_i U_i ; i = 1, 2, ..., n \tag{S.24}$$

$$N_i = \frac{U_i}{U_F} \times 100 \tag{S.25}$$

Where:

U_F : The final utility of the alternative i ,

N_i : The rank score of the option i .

S6 Entropy Shannon weight method

The Shannon entropy method is a commendable concept in information theory, measuring the amount of influential information presented by the criterion system. To acquire the weights of the criteria based on the Shannon entropy values, three main stages should be done, which are elaborated upon hereunder.

1. The decision matrix should be noticed in the first step as introduced in Eq. (S.19). After that, the decision matrix is normalized using Eq. (S.20) to obtain the dimensionless decision matrix X^{χ}.
2. In the second step, the Entropy for each criterion (E_j) was calculated by Eq. (S.26), considering K as the constant value.

$$E_j = -K\sum_{i=1}^{n} x_{ij}^{\chi} \times Ln\left(x_{ij}^{\chi}\right); \forall j, K = \frac{1}{Ln(n)} \tag{S.26}$$

3. In the final step, the deviation degree, d_j, was computed using Eq. (S.27) to present the usefulness of each criterion to the decision-maker. To this extent, different criteria did not differ in terms of their importance when their degrees of deviation were close to each other. Then, the weights of various criteria were calculated by Eq. (S.28).

$$d_j = 1 - E_j; \forall j \tag{S.27}$$

$$W_j = \frac{d_j}{\sum_{j=1}^{m} d_j}; \forall j \tag{S.28}$$

S7 Decision variables ranges

Table S.1 Decision variables range for the MOPSO optimization model

Outlet type	Decision variables	
	Coefficient	Geometry
Orifice	Coefficient (C_O): [0.2,0.8] Correction factor (λ_O): [0.2,0.8]	Cross-sectional area (A_O): [2,10]
Triangular weir	Coefficient (C_T): [0.2,0.8]	Weir's angle (θ_T): [45°,145°]
Rectangular weir	Coefficient (C_R): [0.2,0.8]	Width (L_R): [2,10]
Proportional weir	Coefficient (C_P): [0.2,0.8]	Base distance (s): [0.2,10]

S8 Optimal outlets designs

The optimal values for the hydraulic water head, flood outflow, water deficit, and outlet characteristics were indicated in Tables S.2 to S.5.

Table S.2 The values of Pareto-optimal solutions for the orifice

Sol. #	Hydraulic water head (m)	Flood outflow (m^3/s)	Water deficit (%)	Correction factor (λ_O)	Coefficient (C_O)	Area (A_O)
1	0.013031	1.012105	17.25176	0.47005	0.59155	8.059819
2	0.013264	0.693467	20.01867	0.349085	0.436	10
3	0.01322	0.753326	19.46471	0.457149	0.613742	5.902637
4	0.012956	1.115169	16.45041	0.505161	0.636883	7.697536
5	0.013129	0.878322	18.35796	0.8	0.348072	6.958318
6	0.011742	2.74204	7.687975	0.8	0.8	10
7	0.012471	1.771634	12.26802	0.8	0.501319	10
8	0.013138	0.866468	18.46031	0.609977	0.686789	4.56123
9	0.013343	0.584931	21.0713	0.8	0.8	2
10	0.012901	1.190068	15.88855	0.354737	0.746608	10
11	0.012488	1.74896	12.3927	0.8	0.505948	9.775046
12	0.012172	2.173007	10.18558	0.622505	0.8	10

13	0.013357	0.565427	21.26891	0.486573	0.438967	5.789906
14	0.013688	0.107781	27.76712	0.582183	0.2	2
15	0.013689	0.106784	27.79895	0.2	0.2	5.767826
16	0.01299	1.068868	16.80812	0.389342	0.608869	10
17	0.013585	0.251347	24.8221	0.403656	0.306804	4.40171
18	0.013088	0.934927	17.88075	0.8	0.264438	9.764708
19	0.013587	0.247427	24.87649	0.2	0.441713	6.073687
20	0.012638	1.546203	13.54994	0.799688	0.488315	8.903521
21	0.013556	0.290445	24.28886	0.360438	0.2	8.747289
22	0.012874	1.227113	15.62144	0.480371	0.577815	9.84934
23	0.013647	0.165391	26.22914	0.2	0.367756	4.865837
24	0.013621	0.201297	25.56474	0.2	0.535659	4.069718
25	0.01349	0.382768	23.19629	0.280414	0.502841	5.908034
26	0.013295	0.650697	20.42434	0.678976	0.210091	10
27	0.013002	1.052584	16.93483	0.2923	0.798289	10
28	0.013251	0.710987	19.85448	0.496654	0.314346	10
29	0.012112	2.251897	9.807817	0.646702	0.8	10
30	0.013506	0.359731	23.45543	0.771859	0.305626	3.316812

Table S.3 The values of Pareto-optimal solutions for the proportional weir

Sol. #	Hydraulic water head (m)	Flood outflow (m^3/s)	Water deficit (%)	Coefficient (C_P)	Base distance (s)
1	0.976671	10.23321	1.479707	0.371387	5.951442
2	3.860918	3.457716	0.91386	0.683946	2
3	1.17314	10.01917	1.667205	0.2	8.477953
4	4.61888	1.424646	0.951588	0.2	3.358735
5	4.105321	2.965121	0.742491	0.445929	3.154807
6	3.097442	4.842194	0.691436	0.748983	3.16084
7	0.941215	10.23544	1.43976	0.278758	8.4051
8	0.90772	10.23736	1.398734	0.303491	8.127219
9	0.383572	10.22831	0.869054	0.8	10

10	3.8013	3.99995	0.8892	0.8	2
11	2.920038	2.455489	0.568617	0.25763	5.247748
12	3.898284	3.1985	0.919929	0.62821	2
13	4.197867	2.410986	0.751348	0.319117	3.757881
14	3.297333	2.525977	0.579084	0.282134	4.823797
15	2.534823	2.88032	0.556178	0.304421	5.103048
16	3.643826	4.747355	0.713855	0.8	2.833762
17	4.549634	1.576511	0.876748	0.2	4.001547
18	1.148348	10.21977	1.64794	0.271912	6.6229
19	4.000523	2.396149	1.004774	0.463109	2
20	3.106262	2.962025	0.576583	0.349952	4.48694

Table S.4 The values of Pareto-optimal solutions for the rectangular weir

Sol. #	Hydraulic water head (m)	Flood outflow (m^3/s)	Water deficit (%)	Coefficient (C_R)	Width (L_R)
1	0.661463	10.24507	1.125575	0.650204	5.823844
2	0.707723	10.24461	1.170027	0.8	4.303573
3	0.659003	10.24508	1.123098	0.642435	5.935979
4	0.699488	10.24473	1.162209	0.624127	5.616518
5	0.85358	10.24006	1.324589	0.635766	4.161248
6	0.678489	10.24497	1.142117	0.700569	5.150571
7	1.254345	5.95493	1.33976	0.347892	2.429873
8	1.238742	6.855237	1.443377	0.2	4.99129
9	1.035228	10.22911	1.538888	0.528523	3.881091
10	1.246491	6.09413	1.35295	0.360056	2.430053
11	0.556416	10.24373	1.009735	0.770567	6.185264
12	0.502686	10.24131	0.940396	0.670067	8.219696
13	0.819653	10.24149	1.277366	0.532115	5.317915
14	1.249111	6.354025	1.388508	0.431074	2.099021
15	1.171269	10.21766	1.673542	0.647381	2.673475
16	0.850482	10.2402	1.32002	0.388887	6.945204
17	0.517412	10.24212	0.959624	0.8	6.59681

18	0.68617	10.24489	1.149273	0.512517	7.019145
19	1.054002	10.22769	1.556279	0.558971	3.576549
20	0.947264	10.23507	1.446817	0.627442	3.723311

Table S.5 The values of Pareto-optimal solutions for the triangular weir

Sol. #	Hydraulic water head (m)	Flood outflow (m^3/s)	Water deficit (%)	Coefficient (C_T)	Weir's angle (θ_T)
1	0.327319	1.128256	0.325541	0.733247	79.33699
2	0.313028	0.728231	0.235893	0.2	124.6101
3	0.330204	1.215166	0.343731	0.2772	134.2102
4	0.303715	0.507032	0.178015	0.2	106.3661
5	0.336561	1.420806	0.383075	0.242661	145
6	0.324908	1.057228	0.310189	0.388264	110.6961
7	0.304698	0.528378	0.183927	0.668165	45
8	0.321168	0.950145	0.286356	0.581749	82.46184
9	0.28783	0.188633	0.090111	0.2	51.66777
10	0.310757	0.671426	0.221724	0.2	120.8712
11	0.30072	0.440375	0.15888	0.269206	80.80238
12	0.319079	0.891574	0.273717	0.688901	68.86735
13	0.299105	0.404315	0.148112	0.2	92.73167
14	0.309716	0.645622	0.21516	0.333702	90.82975
15	0.296228	0.346152	0.130229	0.2	83.56243
16	0.291043	0.24586	0.105332	0.2	64.88012
17	0.294815	0.317369	0.121926	0.274454	61.61283
18	0.288853	0.206049	0.095138	0.213833	52.74677
19	0.319658	0.906317	0.276943	0.389901	102.0655
20	0.328824	1.180713	0.336557	0.2	145

S9 Entropy Shannon method results

Table S.6 The Weight results with the Entropy Shannon method

Outlet type	**j**	**Objectives**						
		1	**2**	**3**	**4**	**5**	**6**	**7**
		ID_h	IM_h	$ID_{Q_{out}}$	$IM_{Q_{out}}$	ID_{Def}	IM_{Def}	**Geometry**
Orifice	E_j	0.11337	0.113349	0.104529	0.10481	0.113372	0.111992	0.110994
	d_j	0.88663	0.886651	0.895471	0.89519	0.886628	0.888008	0.889006
	W_j	0.142371	0.142375	0.143791	0.143746	0.142371	0.142593	0.142753
Proportional weir	E_j	0.141499	0.142914	0.141275	0.139478	0.149786	0.146563	0.143735
	d_j	0.858501	0.857086	0.858725	0.860522	0.850214	0.853437	0.856265
	W_j	0.143209	0.142973	0.143246	0.143546	0.141826	0.142364	0.142836
Rectangular weir	E_j	0.146443	0.14764	0.149683	0.149017	0.149786	0.149185	0.146639
	d_j	0.853557	0.85236	0.850317	0.850983	0.850214	0.850815	0.853361
	W_j	0.143176	0.142975	0.142632	0.142744	0.142615	0.142716	0.143143
Triangular weir	E_j	0.148384	0.149731	0.149752	0.142679	0.149787	0.145535	0.147122
	d_j	0.851616	0.850269	0.850248	0.857321	0.850213	0.854465	0.852878
	W_j	0.142721	0.142495	0.142491	0.143677	0.142486	0.143198	0.142932

S10 Ranking results with the COPRAS method for the orifice

Table S.7 showed the ranking for the Pareto-optimal solutions based on the utilities from the COPRAS model to obtain the superior optimal design, wherein the first three prior options were depicted in red. This table showed that the first option for all outlet types had the utility of 1, revealing that these alternatives were the most appropriate optimal solutions. Therefore, as shown in this table, the Pareto-optimal solutions # 14, 19, 17, and 9 were the best answer among alternatives for the superior optimal design of orifice and proportional, rectangular, and triangular weirs, respectively.

Table S.7 Ranking results with the COPRAS method

	Sol. No.	U_i	Rank	Sol. No.	U_i	Rank	Sol. No.	U_i	Rank
Orifice	**1**	0.700178	18	**11**	0.576375	26	**21**	0.820446	10
	2	0.72712	16	**12**	0.526424	28	**22**	0.645438	21
	3	0.777939	12	**13**	0.817748	11	**23**	0.922494	**3**
	4	0.687976	20	**14**	1	**1**	**24**	0.933934	**2**
	5	0.738384	14	**15**	0.908913	6	**25**	0.854578	9
	6	0.471659	30	**16**	0.667075	22	**26**	0.734392	15
	7	0.571645	27	**17**	0.915295	5	**27**	0.669543	20
	8	0.77724	13	**18**	0.690723	19	**28**	0.72417	17
	9	0.886483	7	**19**	0.880287	8	**29**	0.518227	24
	10	0.649135	23	**20**	0.610656	25	**30**	0.913796	4

	Sol. No.	U_i	Rank	Sol. No.	U_i	Rank
Proportional weir	**1**	0.738934	15	**11**	0.92274	13
	2	0.981916	**3**	**12**	0.988787	**2**
	3	0.677554	20	**13**	0.932097	8
	4	0.951996	6	**14**	0.924993	11
	5	0.953755	5	**15**	0.922014	14
	6	0.926802	10	**16**	0.937172	7
	7	0.699254	19	**17**	0.924817	12
	8	0.708261	17	**18**	0.707455	18
	9	0.733925	16	**19**	1	**1**
	10	0.969026	4	**20**	0.930519	9

	Sol. No.	U_i	Rank	Sol. No.	U_i	Rank
Rectangular weir	**1**	0.962855	5	**11**	0.995249	**2**
	2	0.99118	**3**	**12**	0.956885	7
	3	0.960486	6	**13**	0.920216	10
	4	0.954618	8	**14**	0.89417	13
	5	0.938845	9	**15**	0.870232	18
	6	0.976512	4	**16**	0.867497	19
	7	0.886301	15	**17**	1	**1**
	8	0.825666	20	**18**	0.920017	11
	9	0.882228	17	**19**	0.884082	16
	10	0.888027	14	**20**	0.915293	12

	Sol. No.	U_i	Rank	Sol. No.	U_i	Rank
Triangular weir	**1**	0.716105	16	**11**	0.891305	7
	2	0.756526	13	**12**	0.781571	11
	3	0.649976	18	**13**	0.883667	8
	4	0.835156	9	**14**	0.817882	10
	5	0.609292	20	**15**	0.914866	6
	6	0.700178	17	**16**	0.968192	**3**
	7	0.920309	5	**17**	0.960128	4
	8	0.752258	14	**18**	0.996242	**2**
	9	1	**1**	**19**	0.740786	15
	10	0.774315	12	**20**	0.647153	19